Journal of Quantitative Spectroscopy & Radiative Transfer 111 (2010) 357–363

Contents lists available at ScienceDirect

Journal of Quantitative Spectroscopy & Radiative Transfer

journal homepage: www.elsevier.com/locate/jqsrt

Infrared absorption cross sections for ethane (C_2H_6) in the 3 μm region

Jeremy J. Harrison *, Nicholas D.C. Allen, Peter F. Bernath

Department of Chemistry, University of York, Heslington, York YO10 5DD, UK

ARTICLE INFO

Article history:
Received 5 August 2009
Received in revised form
21 September 2009
Accepted 22 September 2009

Keywords:
C_2H_6
Ethane
High-resolution Fourier transform spectroscopy
Infrared absorption cross sections
Remote sensing
Atmospheric chemistry

ABSTRACT

Infrared absorption cross sections for ethane have been measured in the 3 μm spectral region from spectra recorded using a high-resolution FTIR spectrometer (Bruker IFS 125/HR). Results are presented for pure ethane gas from spectra recorded at 0.004 cm^{-1} resolution and for mixtures with dry synthetic air from spectra obtained at 0.015 cm^{-1} resolution (calculated as 0.9/MOPD using the Bruker definition of resolution), at a number of temperatures and pressures appropriate for atmospheric conditions. Intensities were calibrated using three ethane spectra (recorded at 278, 293, and 323 K) taken from the Pacific Northwest National Laboratory (PNNL) IR database.

1. Introduction

Ethane (C_2H_6) is the second most abundant hydrocarbon in the atmosphere, after methane. It was first prepared synthetically in 1834 by Faraday [1] from the electrolysis of a potassium acetate solution, but mistakenly identified as methane. In the late 1840s, Frankland and Kolbe [2] managed to produce ethane, but it was mistaken for the methyl radical. The error was corrected in 1864 by Schorlemmer, who showed experimentally that the product of all these reactions was in fact ethane [3].

Atmospheric ethane has both an anthropogenic and biogenic source with the main emissions being through biomass burning, natural gas loss and biofuel use [4,5]. Ethane is a major component of natural gas and is industrially used as a significant petrochemical feedstock.

The lifetime of ethane in the atmosphere is estimated to be approximately two months [5]. As a consequence concentrations are significantly higher in the lower troposphere. Ethane has a large hemispheric asymmetry with the largest southern hemispheric source attributed to transport from the northern hemisphere [4,6]. The major sink mechanism in the troposphere is through reaction with hydroxyl radicals [7]. The background concentration of ethane has been observed to fluctuate diurnally in synchronisation with the OH radical concentration [8,9]. The predominant destruction mechanism for ethane in the stratosphere is reaction with chlorine atoms [10], however this has been estimated to be only 2% of the global ethane sink [4]. Breakdown products of ethane oxidation include formaldehyde and carbon monoxide [7]. Both ethane and carbon monoxide are found in elevated concentrations within biomass burning plumes [9,11].

Ethane has only a negligible direct radiative forcing effect; however, like many VOCs (volatile organic compounds) it has a significant impact on air quality. Ethane is a strong source of peroxyacetyl nitrate (PAN) in polluted urban air and to a lesser extent in ground level rural air [12]; PAN is a reservoir for nitrogen dioxide. PAN has a major effect on hydroxyl radical and ozone concentrations

* Corresponding author. Tel.: +44 1904 434589; fax: +44 1904 432516.
E-mail address: jjh506@york.ac.uk (J.J. Harrison).

0022-4073/$ - see front matter © 2009 Elsevier Ltd. All rights reserved.
doi:10.1016/j.jqsrt.2009.09.010

[13]. Hence ethane indirectly contributes to the production of tropospheric ozone which is a strong greenhouse gas and is also toxic [14].

Early estimates for ethane emissions varied extensively (see summary in Boissard et al. [15]). Recent estimates for the global emission inventory of ethane using 3D chemical transport models are between 12 and 13.5 Tg yr^{-1} [4,16,17]. Ground based measurements have been taken from sea air [18] and polar firn air [19] to obtain background ethane concentrations. Numerous airborne flask-measurement campaigns over the Pacific and Atlantic oceans, as well as over southern Africa and parts of the Americas [20–22] in the dry season, have investigated biomass burning sources, evolution and transport. Nevertheless these measurements are unable to provide full global coverage.

Ethane is a species of significant interest to astronomers having been identified in the atmospheres of the giant planets and Saturn's moon, Titan. The 3 μm ethane band can be seen in emission in Jupiter's auroral arcs [23]. The Cassini spacecraft has detected light hydrocarbon lakes [24] on the surface of Titan, and ethane (via the 3 μm band) in its atmosphere [25]. There is also evidence for a vast tropospheric ethane cloud at high latitudes [26]. Accurate infrared spectroscopic data are essential for mapping and identifying the important role ethane plays in the complex atmospheric photochemistry observed over Titan. VOCs, including ethane, have also been observed in emission in the 3 μm region of the spectra of several comets [27].

A number of prominent Q branches of the ν_7 band of ethane in the 3 μm region were identified by Coffey et al. from aircraft and ground-based infrared solar absorption spectra [28]. Due to their increased strength compared to Q branches of the ν_9 band at 822 cm^{-1}, this band was identified as being of particular importance for remote-sensing.

First profiles of tropospheric ethane from a low Earth orbit (using a 2976.06–2977.14 cm^{-1} microwindow) were obtained by the Atmospheric Trace Molecule Spectroscopy (ATMOS) Fourier transform spectrometer during the Atmospheric Laboratory for Applications and Science (ATLAS) 3 shuttle flight, 3–12 November 1994 [29].

High-resolution ground-based measurements of ethane have been performed using Fourier transform spectroscopy at both Jungfraujoch [30,31], where total vertical columns were recorded, and in Northern Japan [9] where the outflow of continental air from Asia was monitored.

The Atmospheric Chemistry Experiment (ACE), on board the Canadian satellite SCISAT-1, uses a high-resolution Fourier transform spectrometer for remote sensing of the Earth's atmosphere. This instrument covers the spectral region from 750 to 4400 cm^{-1} [32]. Due to this extended spectral coverage, it is possible to carry out retrievals of ethane in the strong 3 μm region [28,33] using the ν_7 band, where there are fewer spectral interferers than for the ν_9 band (780–868 cm^{-1}), which is used by satellite emission instruments such as MIPAS [34]. Indeed, all aliphatic hydrocarbons have their strongest-intensity modes in the C–H stretching region.

Retrievals of concentration profiles from satellite data require accurate laboratory spectroscopic measurements in the form of either line parameters or absorption cross sections. The HITRAN database is a good source of such spectroscopic data; however the current state of its ethane parameters is rather unsatisfactory in the 3 μm region [35]. Only the nine strongest ^{P}Q branches are currently contained in HITRAN. Brown [36] developed an empirical linelist from unpublished Kitt Peak spectra for these branches in the 2973–3001 cm^{-1} region. Pine and Rinsland [37] subsequently developed a quantum-mechanically based linelist for the $^{P}Q_3$ branch near 2976 cm^{-1}. ^{P}Q branches outside the 2973–3001 cm^{-1} range are not included in HITRAN, and most P and R structure is missing.

ACE currently retrieves ethane using a 2975.5–2977.5 cm^{-1} microwindow, centred on the $^{P}Q_3$ branch. However, ethane is a very strong absorber in the troposphere, and its spectral features in limb spectra tend to dominate those of other VOCs in the 3 μm region. Therefore, the future retrievals of other VOCs with weaker spectral features in this region (assuming that suitable spectroscopic data are available) will require accurate characterisation of ethane over a wider region than currently provided by HITRAN.

In this work we have recorded a new set of high resolution infrared spectra of ethane (with and without additional synthetic air) that cover an appropriate range of temperature and pressure for atmospheric retrievals.

2. Experimental

2.1. Spectrometer

All absorption spectra were recorded at the Molecular Spectroscopy Facility, Rutherford Appleton Laboratory using a high-resolution FTIR spectrometer (Bruker IFS 125/HR) with a KBr beamsplitter, indium antimonide (InSb) detector, and the internal mid-IR radiation source (globar). An optical filter restricted the optical throughput to the spectral region between 2400 and 3500 cm^{-1}. The overall intensity of infrared radiation falling on the InSb detector was therefore maximised in the region of interest without saturating the detector.

2.2. Gas cell

A 26-cm-long single-pass stainless-steel absorption cell, a double-walled cylinder with wedged ZnSe windows sealed on sprung PTFE o-rings, was used for all measurements. The wedged windows eliminate interference fringes (channel spectra) caused by reflections at the surface. The o-ring mounting of the windows is critical to prevent leaks at temperatures down to ~200 K.

The cell was mounted inside the sample compartment of the spectrometer, which was evacuated to < 0.2 Pa in order to minimise the absorbance of impurity gases, and condensation of these gases on the cell windows at the lower measurement temperatures. Cell temperatures below room temperature were achieved

Table 1
Summary of the pressures, temperatures, and instrument parameters for all scans.

Ethane pressure (Torr)	Total pressure (Torr)	Temperature (K)	Resolution (cm^{-1})	Aperture size (mm)	Apodisation function[a]	No. of scans	Scan time (h)[b]
0.0689	0.0689	197	0.004	1.3	NB weak	60	2
0.0765	0.0765	215	0.004	1.3	NB weak	60	2
0.0901	0.0901	250	0.004	1.3	NB weak	60	2
0.1002	0.1002	270	0.004	1.3	NB weak	60	2
0.1124	0.1124	295	0.004	1.3	NB weak	60	2
0.2208	52.13	195	0.015	2.5	NB medium	100	1
0.2220	76.35	195	0.015	2.5	NB medium	100	1
0.2208	103.86	194	0.015	2.5	NB medium	100	1
0.2372	49.44	215	0.015	2.5	NB medium	100	1
0.2389	119.15	215	0.015	2.5	NB medium	100	1
0.4030	206.91	215	0.015	2.5	NB medium	100	1
0.2375	281.11	215	0.015	2.5	NB medium	100	1
0.3066	200.10	250	0.015	2.5	NB medium	100	1
0.2896	400.68	250	0.015	2.5	NB medium	100	1
0.2974	626.45	250	0.015	2.5	NB medium	100	1
0.3029	376.54	270	0.015	2.5	NB medium	100	1
0.3024	601.36	270	0.015	2.5	NB medium	100	1
0.3066	371.71	296	0.015	2.5	NB medium	100	1
0.3058	763.48	297	0.015	2.5	NB medium	100	1

[a] NB=Norton–Beer.
[b] Approximate. Note that each sample spectrum requires a corresponding background spectrum taken with the same spectrometer settings. The scan time is effectively doubled.

by circulating ethanol from a liquid-nitrogen-cooled ethanol bath through the space between the cell walls. The temperature was controlled by regulating the liquid-nitrogen flow via a solenoid valve which was switched by the output of a comparator that compares the temperature in the ethanol bath against a user pre-set temperature. This setup allows automatic temperature control of the cell from ~194 K to room temperature for extended periods of time. The actual cell temperature was monitored by five platinum resistance thermometers (PRTs) in thermal contact at different points on the exterior surface of the cell.

2.3. Sample purity and preparation of gas mixtures

Ethane (99.995% purity) was supplied by Sigma-Aldrich. Synthetic air was provided by Air Products in the form of Air Zero Plus (20.9% $O_2 \pm 0.2\%$, $H_2O \leq 0.5$ ppm, $CH_4 \leq 0.05$ ppm, $CO+CO_2 \leq 0.1$ ppm, 99.99990% overall purity).

Measurements were performed on small amounts of pure ethane as well as on mixtures with dry synthetic air in order to simulate atmospheric pressure-broadened spectra. Mixing ratios were chosen so that self-broadening could be neglected.

Gas handling and pressure measurements were carried out in a gas line, directly attached to the absorption cell. The mixtures of ethane and air were produced by introducing a small amount of ethane directly into the cell and then adding dry synthetic air. Pressures were not measured directly in the cell, but close by, further along the gas line, using full scale 10, 100 and 1000 Torr Baratron capacitance manometers (MKS).

2.4. Recording of spectra

Details of the pressures, temperatures, and instrument parameters for all scans are contained in Table 1. Air-broadened spectra were recorded at 0.015 cm^{-1} resolution, whereas pure gas spectra were recorded at 0.004 cm^{-1} resolution (calculated as 0.9/MOPD using the Bruker definition of resolution). Pre- and post-sample background scans were also recorded as the cell was under vacuum.

2.5. Error budget

The contributions to the errors are given below.

2.5.1. Temperature

The measured average temperature variation of the (outer surface of the) cell was 0.2 K (0.1%) at room temperature and about 1 K (0.5%) at 194 K. Errors for the spanned temperature range varied more or less linearly with temperature.

2.5.2. Pressure

The uncertainties in the pressure readings are estimated to be 0.5%.

Due to the method of preparing ethane/synthetic air mixtures (see above), it is likely that the ethane is not evenly mixed. In particular, some of the ethane left in the gas line is probably forced into the cell when the synthetic air (at substantially higher pressure) is added, resulting in a higher amount of ethane in the cell than indicated by the pressure gauge. We prefer to isolate the cell from the gas line shortly after filling it to decrease the risk of impurities reaching the cell if there are small leaks in the gas line.

Since ethane is the absorbing species, it is particularly important that the amount in the cell is known accurately. This will be considered further in Section 3.1.

Spectra were recorded in blocks of 5 or 10 scans and subsequently co-added, and it was observed that the ethane concentration in the cell did not drop, ruling out any adsorption of ethane onto the cell walls/windows. There was no noticeable leakage of the cell after scans of an hour. Thermal transpiration effects due to the positioning of the pressure gauges relative to the cell and the diameter of the connecting tubing relative to the mean free path of molecules can be safely neglected [38].

2.5.3. Pathlength

The optical pathlength was determined by direct measurement. The overall error is estimated to be 0.1%.

2.5.4. Photometric errors

Photometric errors can arise from problems in determining the exact position of the baseline, i.e. the system response changes from when a background spectrum is taken until when a sample spectrum is measured. These changes might be due to drifts in the light source brightness, detector and electronics response, or changes in the transmittance of the optical path, e.g. impurities.

For these experiments, small changes in the background spectra were noticed with time. It is possible that these changes, which more or less varied linearly with time, were due to organic vapours (outgassing from polymers and pump oil) being deposited on the cell windows. In this work, background (empty cell) spectra were recorded immediately prior to and after the sample spectra. By using averaged backgrounds to calculate the ethane transmittance spectra, most of these changes cancelled. However, the transmission spectra still required small corrections to ensure 100% transmittance outside the ethane absorption band.

A major source of photometric error is the non-linear photometric response of the detector. By using a narrow optical filter to restrict the optical throughput to the spectral region of interest, it was possible to maximise the signal without saturating the detector.

Overall, the photometric uncertainty is estimated to be $\pm 3\%$.

2.5.5. Adsorption

The possibility of ethane adsorbing onto cell walls/windows was ruled out in Section 2.5.2. High purity synthetic air (Section 2.3) was used in these experiments to minimise the adsorption of any impurities, e.g. water vapour, inside the cell at low temperatures. Such impurities could also arise from small leaks in the gas-delivery system. There is no evidence for substantial cell adsorption, however it is very difficult to rule out completely.

2.5.6. Overall uncertainty

The overall uncertainties in the absorption cross sections reported in this paper are estimated to be $\pm 4\%$.

3. Results and discussion

3.1. Data analysis

Transmission spectra were calculated by dividing averaged single-channel sample scans by appropriate single-channel background scans. As mentioned in Section 2.5.4, a further correction was necessary to ensure that the baseline extended to 100% transmittance outside the absorption band. Spectral frequencies were calibrated against an archival Kitt Peak room temperature spectrum of pure ethane, with a small amount of added CO.

The *y*-axes of the cross sections derived in this work were calibrated using spectra from the Pacific Northwest National Laboratory (PNNL) IR database (see http://nwir.pnl.gov). There are several reasons for using PNNL spectra as intensity reference standards. Each PNNL spectrum is a composite of about 10 pathlength-concentration burdens, and great care has been taken to ensure that concentrations are known accurately. For this work, only one spectrum was recorded at each temperature and pressure. Since high-resolution spectra take much longer to record than the lower-resolution PNNL spectra, it was not feasible to take multiple measurements at each temperature and synthetic air pressure for this study.

As outlined in Section 2.5.2, the method used to prepare ethane/synthetic air mixtures resulted in a small discrepancy between the measured ethane pressure and the amount actually in the cell after synthetic air was added. Since cross sections were initially determined using the measured ethane pressure, this calibration procedure effectively normalised the measurements to the true ethane partial pressure within the cell.

Furthermore, it has been demonstrated in the literature that integrated band intensities for isolated bands comprising primarily fundamentals are independent of temperature, or at least show insignificant dependence [39–43]. The spectra in the PNNL database do not extend to temperatures as low as 190 K, but it is a natural consequence of references [39–43] that this independence extends to such low temperatures. Although overtones, combination bands, and hot bands can have small temperature dependences, these are not observed in our measurements or in the PNNL ones (at 278, 293, and 323 K). Integrated band intensities are, of course, independent of the synthetic air pressure, which only modifies the widths of the ethane spectral lines.

The calibration procedure proceeded by converting transmission spectra to PNNL units ($\mathrm{ppm^{-1}\,m^{-1}}$), i.e. the absorbance for a sample concentration of 1 ppm over an optical pathlength of 1 m at 296 K, using the following equation:

$$\varepsilon_{PNNL}(\upsilon, T) = -\frac{T}{296}\frac{0.101325}{Pl}\log_{10}\tau(\upsilon, T) \quad (1)$$

where $\tau(\upsilon, T)$ is the transmittance at wavenumber υ ($\mathrm{cm^{-1}}$) and temperature T (K), P is the pressure of the absorbing gas (Pa), and l is the optical pathlength (m).

All $\varepsilon_{PNNL}(\upsilon, T)$ were integrated between 2545 and 3315 $\mathrm{cm^{-1}}$; the resulting integrals agreed with each other to within 5%. In the PNNL database there are three ethane spectra recorded at 278, 293, and 323 K. These were

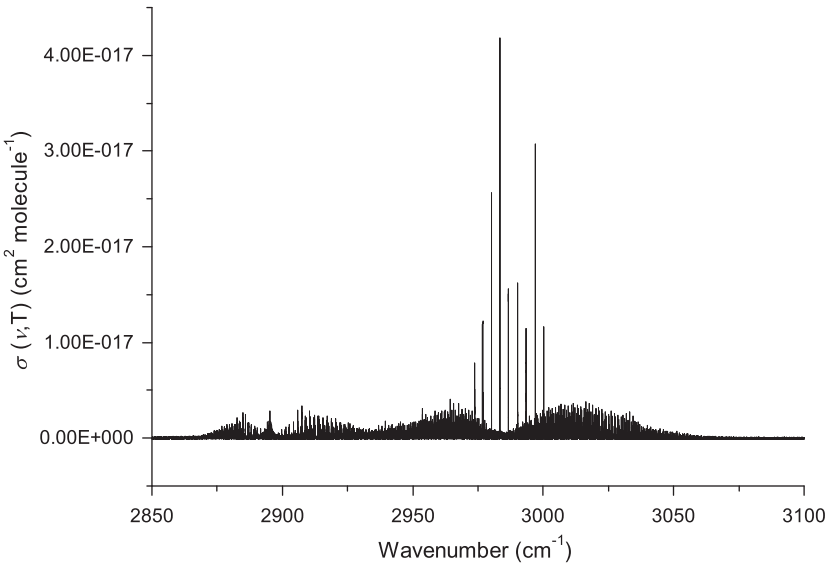

Fig. 1. Absorption cross section data for the 3 μm band of ethane at 215 K.

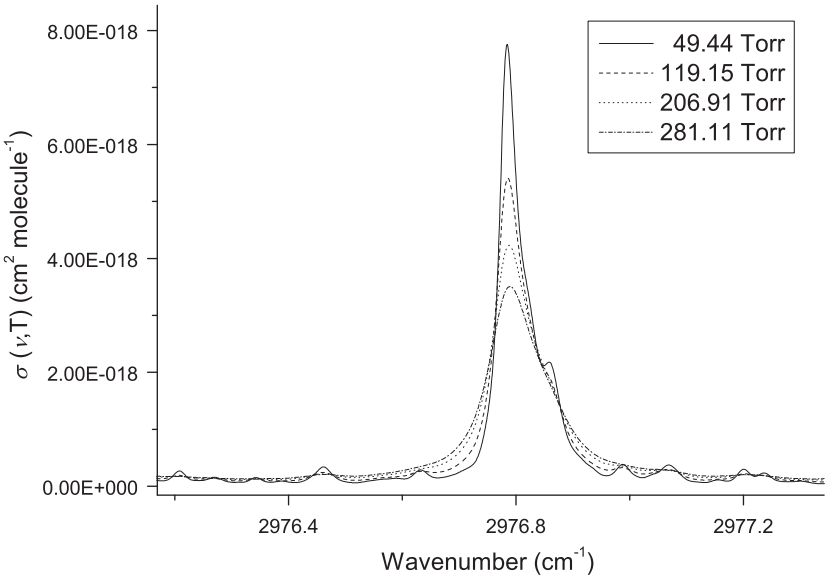

Fig. 2. Absorption cross sections showing the pressure dependence of the $^{P}Q_3$ branch of the 3 μm band of ethane at 215 K.

integrated over the same range (2545–3315 cm^{-1}); the resulting integrals agreed with each other to within 0.5%. All $\varepsilon_{PNNL}(\upsilon, T)$ were calibrated by normalising their integrals against the average of those of ethane from the PNNL database. It was found that the $\varepsilon_{PNNL}(\upsilon, T)$ needed to be reduced by on average 6% to agree with the PNNL data.

Finally, the spectral absorption cross sections, $\sigma(\upsilon,T)$, with units cm^2 $molecule^{-1}$, were calculated by

$$\sigma(\upsilon,T) = -\xi\frac{10^4 k_B T \ln\tau(\upsilon,T)}{Pl} \quad (2)$$

where k_B is the Boltzmann constant (=1.3806504×10^{-23} JK^{-1}) and ξ is the factor required to scale each spectrum to PNNL values. All other symbols (and corresponding units) are as defined for Eq. (1). A selection of cross sections is given in Figs. 1 and 2. The first figure gives an overview of the entire ethane 3 μm band at 215 K, whereas the second shows the pressure dependence of the $^{P}Q_3$ branch. All the spectral absorption cross sections corresponding to the experimental conditions in Table 1 are available electronically upon request from the authors.

3.2. ACE retrievals

Version 3.0 ethane retrievals (using the HITRAN linelist) for two ACE occultations (ss11613 and ss4786) were

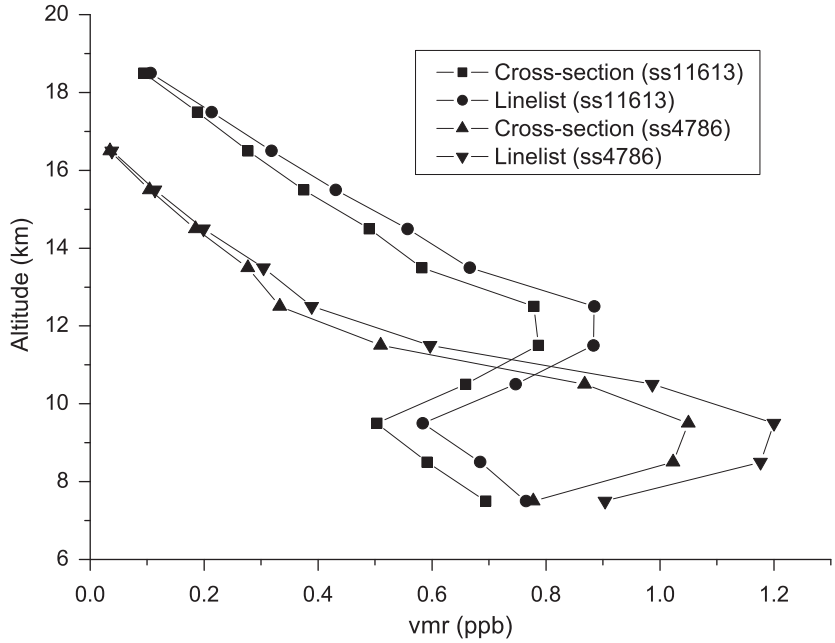

Fig. 3. Plots of version 3.0 ethane retrievals for two ACE occultations (ss11613 and ss4786) using both the HITRAN linelist and the new cross sections over the same microwindow (2975.5–2977.5 cm^{-1}). Note that retrievals using the cross sections are consistently lower than those using the linelist.

compared to ethane retrievals using the new cross sections over the same microwindow (2975.5–2977.5 cm^{-1}). As can be seen in Fig. 3, in which volume mixing ratio (vmr; in ppb) is plotted against altitude (in km), retrievals using the new cross sections are consistently lower than those using the HITRAN linelist. In fact, for these two occultations, the vmrs are on average 11.6% lower and the corresponding standard deviations 13.2% lower. Since the new cross sections are consistent with PNNL in terms of intensity, we are confident of their accuracy.

Unfortunately, these new cross sections suggest that previous and current operational ACE ethane retrievals are too high. It is planned to update and optimise these retrievals by updating and improving the microwindow set. This reinforces the need of satellite remote-sensing missions for accurate laboratory spectroscopic data.

4. Conclusions

High-resolution infrared absorption cross sections for ethane (between 2545 and 3315 cm^{-1}) have been measured with an estimated overall uncertainty of about 4%. The data were recorded for the pure gas at 0.004 cm^{-1} resolution and for mixtures with dry synthetic air at 0.015 cm^{-1} resolution using a range of temperatures and pressures appropriate for atmospheric conditions. Intensities were calibrated against three ethane spectra taken from the PNNL IR database. These cross sections will be used to obtain more accurate ethane retrievals from ACE solar occultation spectra than currently possible using the rather incomplete line parameters from the HITRAN database. They will also enable the retrieval in the 3 μm region of other VOCs with weaker spectral features that are easily dominated by those of ethane.

Acknowledgements

The authors wish to thank the Natural Environment Research Council (NERC) for supporting J.J. Harrison through Grant NE/F002041/1 and N.D.C. Allen through the National Centre for Earth Observation (NCEO), and for access to the Molecular Spectroscopy Facility (MSF) at the Rutherford Appleton Laboratory (RAL). R.G. Williams is thanked for providing technical support at the RAL. The ethane data was recorded as part of a proposal to the MSF entitled "Low temperature, high resolution spectroscopy in the 3, 7 and 11.7 μm bands of ethane and propane gas" by N. Bowles, J.J. Remedios and P.F. Bernath. We also thank R.J. Parker for assistance with some of the early ethane measurements that were ultimately not used because of leaks in the absorption cell. C.D. Boone and S.D. McLeod from the University of Waterloo, Canada, are thanked for assistance with ACE retrievals. ACE is supported primarily by the Canadian Space Agency.

References

[1] Faraday M. Experimental research in electricity-—seventh series. Phil Trans R Soc Lond 1834;124:77–122.
[2] Kolbe H, Frankland E. On the products of the action of potassium on cyanide of ethyl. Q J Chem Soc 1849;1:60–74.
[3] Schorlemmer C. On the identity of methyl and hydride of ethyl. J Chem Soc 1864;17:262–5.
[4] Xiao Y, Logan JA, Jacob DJ, Hudman RC, Yantosca R, Blake DR. Global budget of ethane and regional constraints on US sources. J Geophys Res 2008;113(D21306) doi:10.1029/2007JD009415.

[5] Rudolph J. The tropospheric distribution and budget of ethane. J Geophys Res 1995;100(D6):11,369–81.
[6] Blake DR, Rowland FS. Global atmospheric concentrations and source strength of ethane. Nature 1986;321:231–3.
[7] Aikin AC, Herman JR, Maijer EJ, Mcquillan CJ. Atmospheric chemistry of ethane and ethylene. J Geophys Res 1982;87(C4): 3105–3118.
[8] Jobson BT, Parrish DD, Goldan P, Kuster W, Fehsenfeld FC, Blake, DR, et al. Spatial and temporal variability of nonmethane hydrocarbon mixing ratios and their relation to photochemical lifetime. J Geophys Res 1998;103(D11):13557–67.
[9] Zhao Y, Strong K, Kondo Y, Koike M, Matsumi Y, Irie, H, et al. Spectroscopic measurements of tropospheric CO, C_2H_6, C_2H_2, and HCN in northern Japan. J Geophys Res 2002;107(D18):4343, doi:10.1029/2001JD000748.
[10] Chameides WL, Cicerone RJ. Effects of nonmethane hydrocarbons in the atmosphere. J Geophys Res 1978;83(C2):947–52.
[11] Greenberg JP, Zimmerman PR, Heidt L, Pollock W. Hydrocarbon and carbon monoxide emissions from biomass burning in Brazil. J Geophys Res 1984;89(D1):1350–4.
[12] Singh HB, Hanst PL. Peroxyacetyl nitrate (PAN) in the unpolluted atmosphere: an important reservoir for nitrogen oxides. Geophys Res Lett 1981;8(8):941–4.
[13] Kanakidou M, Singh HB, Valentin KM, Crutzen PJ. A two-dimensional study of ethane and propane oxidation in the troposphere. J Geophys Res 1991;96(D8):15,395–413.
[14] Gupta ML, Cicerone RJ, Blake DR, Rowland FS, Isaksen ISA. Global atmospheric distributions and source strengths of light hydrocarbons and tetrachloroethene. J Geophys Res 1998;103(D21): 28219–28235.
[15] Boissard C, Bonsang B, Kanakidou M, Lambert G. TROPOZ II: global distributions and budgets of methane and light hydrocarbons. J Atmos Chem 1996;25:115–48.
[16] Xiao Y, Jacob DJ, Wang JS, Logan JA, Palmer PI, Suntharalingam, P, et al. Constraints on Asian and European sources of methane from CH_4–C_2H_6–CO correlations in Asian outflow. J Geophys Res 2004;109(D15S16) doi:10.1029/2003JD004475.
[17] Stein O, Rudolph J. Modeling and interpretation of stable carbon isotope ratios of ethane in global chemical transport models. J Geophys Res 2007;112(D14308) doi:10.1029/2006JD008062.
[18] de Gouw JA, Middlebrook AM, Warneke C, Goldan PD, Kuster WC, Roberts, JM, et al. Budget of organic carbon in a polluted atmosphere: results from the New England air quality study in 2002. J Geophys Res 2005;110(D16305) doi:10.1029/2004JD005623.
[19] Kaspers KA, van de Wal RSW, de Gouw JA, Hofstede CM, van den Broeke MR, van der Veen, C, et al. Analyses of firn gas samples from Dronning Maud Land, Antarctica: study of nonmethane hydrocarbons and methyl chloride. J Geophys Res 2004;109(D02307) doi:10.1029/2003JD003950.
[20] Blake NJ, Blake DR, Simpson IJ, Meinardi S, Swanson AL, Lopez, JP, et al. NMHCs and halocarbons in Asian continental outflow during the transport and chemical evolution over the Pacific (TRACE-P) field campaign: comparison with PEM-West B. J Geophys Res 2003;108(D20):8806–30.
[21] Blake NJ, Blake DR, Sive BC, Chen T-Y, Rowland FS, Collins Jr. JE, et al. Biomass burning emissions and vertical distribution of atmospheric methyl halides and other reduced carbon gases in the South Atlantic region. J Geophys Res 1996;101(D19):24,151–64.
[22] Blake NJ, Blake DR, Wingenter OW, Sive BC, McKenzie LM, Lopez, JP, et al. Influence of southern hemispheric biomass burning on midtropospheric distributions of nonmethane hydrocarbons and selected halocarbons over the remote South Pacific. J Geophys Res 1999;104(D13):16213–32.
[23] Kim SJ, Geballe TR, Seo HJ, Kima JH. Jupiter's hydrocarbon polar brightening: discovery of 3-micron line emission from south polar CH_4, C_2H_2, and C_2H_6. Icarus 2009;202:354–7.
[24] Brown RH, Soderblom LA, Soderblom JM, Clark RN, Jaumann R, Barnes, JW, et al. The identification of liquid ethane in Titan's Ontario Lacus. Nature 2008;454(7204):607–10.
[25] Hesman BE, Jennings DE, Sada PV, Bjoraker GL, Achterberg RK, Simon-Miller, A-A, et al. Saturn's latitudinal C_2H_2 and C_2H_6 abundance profiles from Cassini/CIRS and ground-based observations. Icarus 2009;202:249–59.
[26] Griffith CA, Penteado P, Rannou P, Brown R, Boudon V, Baines, KH, et al. Evidence for a polar ethane cloud on titan. Science 2006;313:1620–2.
[27] Böhnhardt H, Mumma MJ, Villanueva GL, DiSanti MA, Bonev BP, Lippi, M, et al. The unusual volatile composition of the Halley-type comet 8P/Tuttle: addressing the existence of an inner Oort Cloud. Astrophys J 2008;683:L71–4.
[28] Coffey MT, Mankin WG, Goldman A, Rinsland CP, Harvey GA, Malathy Devi, V, et al. Infrared measurements of atmospheric ethane (C_2H_6) from aircraft and ground-based solar absorption spectra in the 3000 cm^{-1} region. Geophys Res Lett 1985;12(4): 199–202.
[29] Rinsland CP, Gunson MR, Wang PH, Arduini RF, Baum BA, Minnis, P, et al. ATMOS/ATLAS 3 infrared profile measurements of trace gases in the November 1994 tropical and subtropical upper troposphere. JQSRT 1998;60(5):891–901.
[30] Mahieu E, Zander R, Delbouille L, Demoulin P, Roland G, Servais C. Observed trends in total vertical column abundances of atmospheric gases from IR solar spectra recorded at the Jungfraujoch. J Atmos Chem 1997;28:227–43.
[31] Rinsland CP, Mahieu E, Zander R, Demoulin P, Forrer J, Buchmann B. Free tropospheric CO, C_2H_6, and HCN above central Europe: recent measurements from the Jungfraujoch station including the detection of elevated columns during 1998. J Geophys Res 2000;105(D19):24,235–249.
[32] Bernath PF, McElroy CT, Abrams MC, Boone CD, Butler M, Camy-Peyret, C, et al. Atmospheric Chemistry Experiment (ACE): mission overview. Geophys Res Lett 2005;32(L15S01) doi:10.1029/2005GL022386.
[33] Rinsland CP, Dufour G, Boone CD, Bernath PF, Chiou L. Atmospheric Chemistry Experiment (ACE) measurements of elevated Southern Hemisphere upper tropospheric CO, C_2H_6, HCN, and C_2H_2 mixing ratios from biomass burning emissions and long-range transport. J Geophys Res 2005;32:L20803, doi:10.1029/2005GL024214.
[34] von Clarmann T, Glatthor N, Koukouli ME, Stiller GP, Funke B, Grabowski, U, et al. MIPAS measurements of upper tropospheric C_2H_6 and O_3 during the southern hemispheric biomass burning season in 2003. Atmos Chem Phys 2007;7:5861–72.
[35] Rothman LS, Gordon IE, Barbe A, Benner DC, Bernath PF, Birk, M, et al. The HITRAN 2008 molecular spectroscopic database. JQSRT 2009;110:533–72.
[36] Brown LR, Farmer CB, Toth RA, Rinsland CP. Molecular line parameters of the Atmospheric Trace Molecule Spectroscopy Experiment. Appl Opt 1987;26:5154–82.
[37] Pine AS, Rinsland CP. The role of torsional hot bands in modeling atmospheric ethane. JQSRT 1999;62:445–58.
[38] Takaishi T, Sensui Y. Thermal transpiration effect of hydrogen, rare gases and methane. Trans Faraday Soc 1963;59:2503–14.
[39] Crawford Jr. B. Vibrational intensities: integration theorems. J Chem Phys 1958;29:1042–5.
[40] Mills IM, Whiffen DH. Integration theorems on vibrational intensities. J Chem Phys 1959;30:1619–20.
[41] Breeze JC, Ferriso CC, Ludwig CB, Malkmus W. Temperature dependence of the total integrated intensity of vibrational-–rotational band systems. J Chem Phys 1965;42:402–6.
[42] Yao SJ, Overend J. Vibrational intensities: effect of anharmonicity on temperature-dependence of integrated intensities. Spectrochim Acta 1976;32:1059–65.
[43] Sams RL, Sharpe SW, Johnson TJ. Do Integrated Infrared Band Strengths Change with Temperature in the Gas-Phase? Do integrated infrared band strengths change with temperature in the gas-phase? In: Presentation, 60th International Symposium on Molecular Spectroscopy (2005) at, Columbus, Ohio, US, 2005.